Dynamics in Miscible Blends of Polystyrene and Poly(vinyl methyl ether)

Jai A. Pathak,[†] Ralph H. Colby,*[,‡] George Floudas,[§] and Robert Jérôme[||]

Departments of Chemical Engineering and Materials Science and Engineering, The Pennsylvania State University, University Park, Pennsylvania 16802, Foundation for Research and Technology−Hellas (FORTH), Institute of Electronic Structure and Laser, P.O. Box 1527, 711 10 Heraklion, Crete, Greece, and Center for Education and Research on Macromolecules (CERM), University of Liège, Sart-Tilman, B6, 4000 Liège, Belgium

Received November 4, 1998; Revised Manuscript Received February 9, 1999

ABSTRACT: We report results on the linear viscoelasticity (oscillatory shear in the temperature range T_g (glass-transition temperature) $\leq T \leq T_g + 90$ K) of miscible blends of polystyrene (PS) and poly(vinyl methyl ether) (PVME) and segmental relaxations, measured by dielectric spectroscopy. The Flory−Huggins interaction parameter of this blend is weakly negative, and the glass transitions of the pure components are quite disparate ($\Delta T_g = 125$ K). PS/PVME blends have been found to be *consistently thermorheologically complex at both the segmental and terminal levels*: the empirical time−temperature superposition (tTS) principle applies to neither their oscillatory shear response nor their dielectric response. Using the tube model, we quantitatively compare dielectric and mechanical results. At low temperatures, the effective time scale for motion of a Kuhn segment (the shortest Rouse mode) is near the long-time end of the distribution of segmental relaxation times of PVME, in both the pure and blended states. The slowest relaxing segments thus control the longer-time relaxation processes of the chains. Miscible blends with weak interactions and large ΔT_g have concentration fluctuations that broaden the distribution of segmental relaxation times. This distribution narrows as the temperature is raised in the blend, leading to the failure of tTS for terminal dynamics.

1. Introduction

There has recently been a surge of academic and industrial interest in polymer blends,[1,2] and their rheology is of paramount importance for processing. Empirical relations for the composition dependence of blend viscosity exist,[2] but they are kept too general to be useful for predictions to account for both large positive and negative deviations from additivity of log η.

The empirical time−temperature superposition (tTS) principle[3] breaks down in miscible blends of polymers with very different glass-transition temperatures.[4−13] This thermorheological complexity has been seen for both terminal (whole chain) relaxations[4,6,7,10−12] and for segmental relaxations.[5,8,9,14−18] However, comparisons of the complexity at the segmental and terminal levels have only been made for the polyisoprene/polyvinylethylene system.[19]

Here, we investigate miscible blends of polystyrene (PS) and poly(vinyl methyl ether) (PVME). The pure components have very different glass-transition temperatures, $\Delta T_g = 125$ K, making this blend have *large dynamic asymmetry*. The χ parameter of PS/PVME is weakly negative.[20−22] Kumar et al.[13,17] predict that, in the absence of strong specific interactions, a miscible polymer blend with such a large ΔT_g should be thermorheologically complex. In this paper, we study the thermorheological complexity of PS/PVME blends at both the segmental level using dielectric spectroscopy (DS) and over a range extending from the segmental level to the terminal (whole chain relaxation) level using oscillatory shear (OS) rheometry. Although both PVME and PS have dipole moments, the dipole moment of PVME greatly exceeds that of PS,[14,23] so we focus on the segmental motion of the PVME chains in DS. We first discuss the results of each technique separately and then make a quantitative comparison of DS and OS in the Discussion.

2. Background

2.1. Thermodynamics. Phase behavior and thermodynamics in PS/PVME blends have been extensively studied. Differential scanning calorimetry (DSC) and DS experiments indicate that atactic PS and PVME form miscible mixtures with each other.[24−27] Syndiotactic and isotactic PS mixtures with a PVME phase separate at all temperatures above the T_g of PVME.[28,29] 2-D NMR experiments by Mirau and co-workers[30−32] on PS/PVME blends suggest there are weak van der Waals interactions between the PS phenyl ring and the PVME methoxyl group, consistent with the weakly negative value of the χ parameter observed in SANS experiments.[20−22,33−39] PS/PVME has a negative enthalpy of mixing,[40,41] a small negative volume change on mixing,[41] and a lower critical solution temperature.[26]

2.2. Dynamics. Both oscillatory and steady shear have been used to investigate the rheology of PS/PVME single-phase blends.[42−52] In addition, Green and coworkers have examined the temperature and composition dependence of the tracer diffusion coefficient of *d*-PS in PS/PVME blends by forward recoil spectroscopy.[53,54]

The applicability of tTS to the viscoelastic response of PS/PVME blends is debated in the literature. Cavaille et al.[43] and Stadler et al.[45] have constructed master curves of tan $\delta \equiv G''/G'$ and arrived at the conclusion that the blend shows departures from tTS. However, the opposite conclusion of thermorheological simplicity

[†] Chemical Engineering, Penn State.
[‡] Materials Science and Engineering, Penn State.
[§] Foundation for Research and Technology-Hellas.
[||] CERM, University of Liège.

10.1021/ma9817121 CCC: $18.00
Published on Web 03/31/1999

Table 1. Molecular Characteristics of Polymers

polymer	M_w	M_w/M_n
PVME	124 000	1.25
PS-50	52 000	<1.1
PS-130	131 000	1.2
PS-260	263 000	<1.1

has been drawn when only master curves of G' and G'' are constructed.[47,51,52] However, these studies were focused on rheology in the two-phase region, and most of the single-phase rheology only included terminal response, where tTS works by default.

Dielectric studies of the α-relaxation of PVME[14,15,23,55] in PS/PVME blends indicate thermorheological complexity. The α-relaxation of PVME broadens significantly when blended with PS, and the segmental relaxation time distribution in the blend narrows as the temperature is raised. Concentration fluctuations are believed to be responsible for both the broadening and the failure of tTS in PS/PVME blends.[14,15,55]

Several solid-state NMR studies on PS/PVME blends indicate a spatial distribution of mobility. Cross polarization experiments[56] (from ^{1}H to ^{13}C) indicate that, although most of the PVME is quite mobile 60 K above the blend T_g, the PS chains have a broad distribution of mobilities that are generally much slower than those of PVME. The ^{2}H NMR spectra of *d*-PS/PVME blends[57] clearly show the superposition of immobile PS (with quadrupole splittings of the solid state) and mobile PS (with a sharp central peak characteristic of a liquid), with a larger fraction of mobile PS as the temperature increases.

3. Experimental Section

3.1. Materials, Characterization, and Blend Preparation. Size-exclusion chromatography in THF was used to determine the weight-average molecular weights (M_w) of the PS and PVME (relative to PS) and polydispersities (M_w/M_n), where M_n denotes the number-average molecular weight (Table 1). Three anionically polymerized PS samples were obtained from three different sources (PS-50 was obtained from T. E. Long, PS-130 was obtained from R. Stadler, and PS-260 was obtained from Scientific Polymer Products of Ontario, NY).

The PVME was synthesized by cationic polymerization at CERM. The methyl vinyl ether monomer was supplied by Matheson. Hydrogen iodide (57% aqueous solution) and zinc iodide (99.99% purity) were obtained from Aldrich. Toluene was refluxed over CaH_2 and distilled. Just prior to reaction, the toluene was distilled over a polystyryllithium solution. HI from aqueous solution was dissolved in dry *n*-hexane according to a published procedure.[58] Diethyl ether was dried by refluxing over metallic sodium and distilled. Methyl vinyl ether was purified by distilling the condensed monomer over polystyryllithium solution. ZnI (cocatalyst) was dissolved in dry ether (0.16 M). Dry toluene was introduced into a flame-treated flask, under nitrogen, followed by freshly distilled monomer. The solution was cooled to −40 °C, before the calculated quantity of hydrogen iodide and zinc iodide (1:1 molar ratio) was added. Polymerization was allowed to proceed for 4 h at −40 °C and then for 7 days at −15 °C. The reaction was quenched with prechilled ammoniacal methanol. The polymer solution was washed with both a 10% aqueous sodium thiosulfate solution and water. The organic layer was dried with anhydrous sodium sulfate, and the solvent was removed under reduced pressure leaving the polymer (80% yield).

The PVME was fractionated in two stages. A 5% solution in demineralized water was heated to 60 °C, where a precipitate formed. The solution was decanted and reheated to 60 °C, where a second precipitate was collected. A 3% solution of these two fractions (combined) was heated to 40 °C, where a precipitate formed. The solution was decanted and reheated to 40 °C, where a second precipitate was collected. These two precipitates were combined to make the PVME used in this study. Size-exclusion chromatography indicates that the fractionation narrowed the molecular weight distribution from $M_w/M_n = 1.5$ before fractionation to $M_w/M_n = 1.25$ after fractionation.

All blends were prepared by dropwise precipitation of a toluene solution of the two polymers into a 20-fold excess of *n*-heptane (nonsolvent) at −78 °C. The stringy white precipitate was filtered cold and then dried in a vacuum oven, first at 80 °C for 2 days and then at room temperature for approximately 1 month, until its weight loss was less than 0.01 g in one week.

The glass-transition temperatures of the pure polymers are listed in Table 2, as determined by differential scanning calorimetry on a Seiko Instruments SSC 5200 DSC, with 5−10 mg of sample. The DSC was calibrated with an indium standard, which melts at 156.6 °C. Heating and cooling rates of 10 K/min were consistently used for all samples, and only the data from the second heating were used to determine the T_g (defined to be the temperature at the midpoint of the transition). All blends investigated have a single calorimetric glass transition, intermediate to the glass transitions of the pure components ($T_g = 3$ °C for 30% PS/70% PVME blends and $T_g = 25$ °C for 50% PS/50% PVME blends). This feature and optical clarity were taken as necessary evidence for miscibility. Samples were prepared for both OS and DS by molding overnight in vacuum-assisted compression molds, at 60−80 °C. The PVME and all blends showed small amounts of a crystalline component, if annealed at room temperature for an extended period (>1 week). The crystals melt at 50 °C. For this reason, OS was measured on freshly molded samples. The loading procedure for DS requires heating the samples in excess of 50 °C, so it was not surprising that there was no indication of any crystallinity in either the DS or OS experiments.

3.2. Rheology. Oscillatory shear rheometry was performed at Pennsylvania State University on all blends and pure components in a Rheometric Scientific ARES rheometer, which was equipped with a force-rebalance transducer and capable of measuring torque signals between 0.2 and 2000 g cm. The applied strain amplitudes ($0.001 < \gamma_0 < 0.1$) were always less than the maximum strain for producing linear viscoelastic response, as determined by strain sweeps at various frequencies. For experiments between T_g and $T_g + 30$ K, 7.9 mm diameter parallel plates were used, whereas 25 mm diameter parallel plates were used at higher temperatures. Temperature was controlled by a steady flow of heated nitrogen gas through the sample chamber. Frequencies between 10^{-2} and 10^2 rad/s were typically used, although slightly lower frequencies (of order 10^{-3} rad/s) were used in some experiments to measure viscoelastic response on longer time scales.

3.3. Dielectric Spectroscopy. The DS measurements were made at FORTH on PVME, PS-130 and two blends. All samples were identical to the ones used in the OS investigation. Measurements of the complex dielectric function were made with a Novocontrol BDC-S system composed of a frequency response analyzer (Solartron Schlumberger FRA 1260) and a broadband dielectric converter with an active sample cell. The latter contains six reference capacitors in the range from 25 to 1000 pF. Measurements were made in the frequency range from 10^{-2} to 10^6 Hz using a combination of three capacitors in the active sample cell. The resolution in $\tan\delta$ was about 2×10^{-4} in the frequency range between 10^{-1} to 10^5 Hz. The samples were kept between two 20 mm diameter gold-plated stainless steel plates with a separation of 100 μm, which resulted in a sample capacitance of about 100 pF. The sample cell was set in a cryostat and the sample temperature was controlled between 240 and 340 K with an accuracy of ±0.1 K.

4. Oscillatory Shear Master Curves

The tTS principle[3] allows the frequency ω dependence of the complex modulus G^* at any temperature T to be

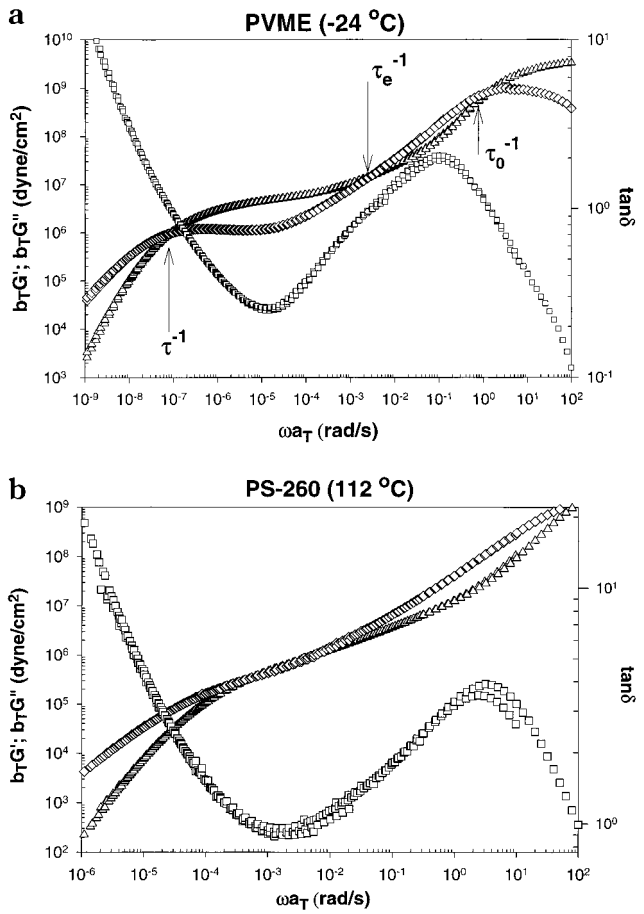

Figure 1. Master curves of the storage modulus (G', triangles), loss modulus (G'', diamonds), and the loss tangent (tan δ, squares) for two pure components: (a) PVME referenced to −24 °C (=T_g) using data at −24, −14, −4, 6, 16, 26, 36, 46, and 56 °C and (b) PS-260 referenced to 112 °C (= T_g + 6 K) using data at 112, 116, 126, 136, 146, and 156 °C. The arrows in (a) show the frequencies that are reciprocals of the terminal relaxation time τ, the Rouse time of an entanglement strand τ_e, and the relaxation time of a Kuhn segment τ_0. τ_e and τ_0 were estimated from τ, as described in the Discussion.

determined from a master curve at a reference temperature, which we take to be the glass transition T_g.

$$G^*(\omega; T) = b_T G^*(a_T\omega; T_g) \quad (1)$$

At each temperature T, a single frequency-scale shift factor a_T and a single (much smaller) modulus-scale shift factor b_T allow superposition of all viscoelastic data at temperature T with the data at the reference temperature T_g.

Our superposition procedure involves first shifting the loss tangent tan δ on the frequency scale (determining a_T) and subsequently determining b_T by an independent modulus-scale shift of G^*. This procedure separates the two shifts because the loss tangent is the ratio of G'' to G''.

$$\tan\delta = G''/G' \quad (2)$$

Representative master curves of G', G'' and tan δ for the pure component polymers are shown in Figure 1 for PVME (Figure 1a) and PS-260 (Figure 1b). (The force-rebalance transducer starts to exhibit compliance effects with 7.9 mm diameter plates at modulus levels exceeding 10^9 dynes/cm^2. Thus, the data in Figure 1a for frequencies ωa_T > 3 rad/s are only qualitatively correct.)

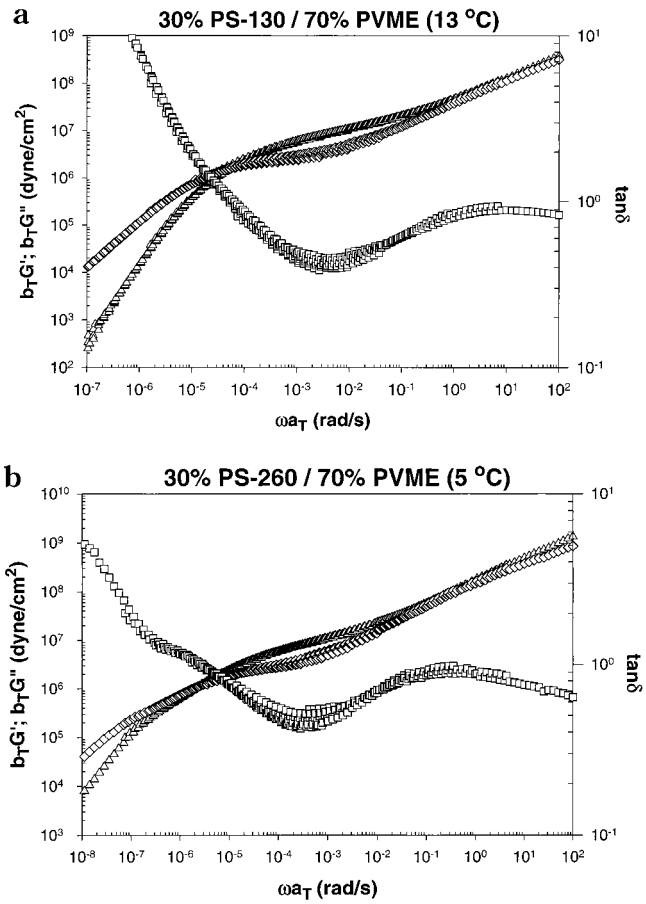

Figure 2. Master curves of the storage modulus (G', triangles), loss modulus (G'', diamonds), and the loss tangent (tan δ, squares) for two blends: (a) 30/70 wt % PS-130/PVME referenced to 13 °C (= T_g + 10 K) using data at 13, 23, 33, 43, 53, 63, 73, 83, and 93 °C and (b) 30/70 wt % PS-260/PVME referenced to 5 °C (= T_g + 2 K) using data at 5, 15, 25, 35, 45, 55, 65, and 75 °C.

The frequency-scale shifts for the pure components follow the Williams−Landel−Ferry (WLF) equation[3] (discussed below). Superposition of the tan δ master curves for PVME is typical of OS results on homopolymer melts,[13,59,60] where tTS works reasonably for all temperatures above T_g. Plazek[61,62] has reported that tTS fails for PS between 97.0 and 114.5 °C (corroborated by Cavaille et al.[43]). Our data on pure PS show tTS working only approximately for PS at $T > T_g$ + 10 K. At lower temperatures (T_g + 6 K), a clear breakdown of tTS is seen in PS-260.

Representative G', G'', and tan δ master curves for the blends are shown in Figure 2 for the 30/70 wt % PS-130/PVME blend (Figure 2a) and the 30/70 wt % PS-260/PVME blend (Figure 2b). All PS/PVME blends studied show a clear breakdown of tTS.

5. Dielectric Spectroscopy Master Curves

The time−temperature superposition principle is also used to make master curves of the frequency ν dependence of the complex permittivity ϵ^* determined by DS.[63]

$$\epsilon^*(\nu; T) = c_T\epsilon^*(a_T\nu; T_g) \quad (3)$$

The dielectric constant scale temperature shift factor c_T is always of order unity. For PVME, we find that c_T < b_T and that c_T fits the standard Clausius−Mosotti

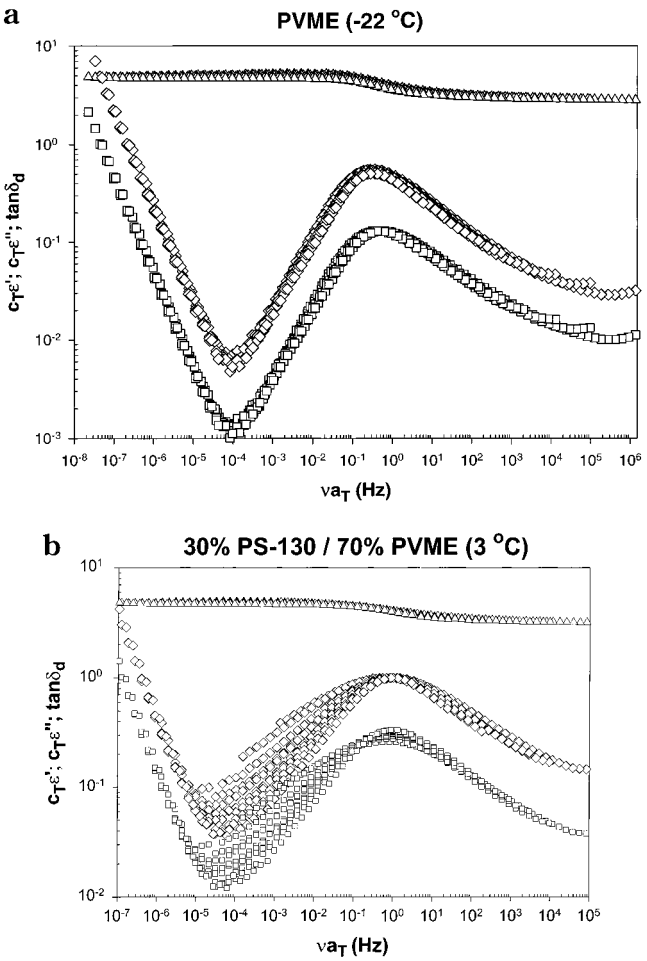

Figure 3. Master curves of the dielectric storage (ϵ', triangles), dielectric loss (ϵ'', diamonds), and the dielectric loss tangent (tan δ_d, squares): (a) pure PVME referenced to −22 °C (= T_g + 2 K), using data at −22, −17, −12, −7, −2, 3, 8, 13, 18, 23, and 28 °C and (b) 30/70 wt % PS-130/PVME referenced to 3 °C (= T_g) using data at −7, −2, 3, 8, 13, 23, 28, 33, and 38 °C.

form[64] of eq 4 for the low-frequency limiting permittivity ϵ_0, where $\rho(T)$ is the (temperature-dependent) density[40] and A is the (temperature-independent) specific polarizability of PVME.

$$\epsilon_0(T) = \frac{1 + 2\rho(T)A}{1 - \rho(T)A} \tag{4}$$

Fitting our measured c_T for PVME to eq 4, we conclude that the specific polarizability of PVME is $A = 0.62$ cm^3/g.

Time−temperature superposition was applied successfully to the DS data for pure PVME by preparing master curves of tan $\delta_d \equiv \epsilon''/\epsilon'$. Master curves of tan δ_d, ϵ', and ϵ'', shown in Figure 3a, are obtained from superposition of data in temperature increments of 5 K, between −22 and +28 °C.

The tan δ_d master curve of the 30/70 wt % PS-130/PVME blend, shown in Figure 3b, reveals an obvious failure of tTS. The attempted master curves in Figure 3b were prepared from complex permittivity data at temperatures ranging from −7 to +38 °C, in temperature increments of 5 K. Segmental motion of the PVME chains dominate the dielectric response of the blend because the specific polarizability of PS is much smaller than PVME. Figure 3b shows that the distribution of

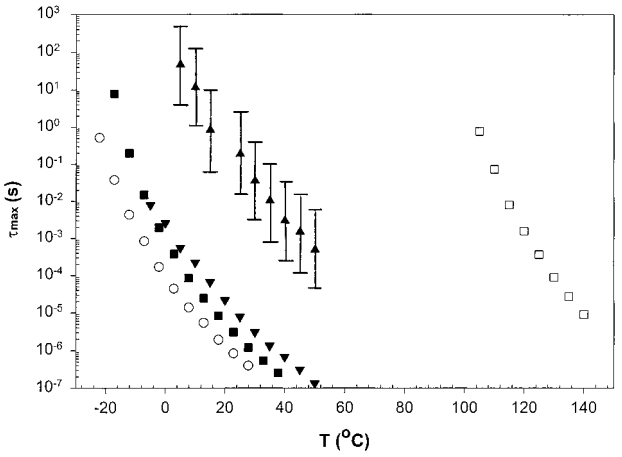

Figure 4. Temperature dependence of segmental relaxation times extracted from dielectric spectroscopy data for PS-130 (open squares), PVME (open circles), 30/70 wt % PS-130/PVME blend (filled squares), and 50/50 wt % PS-50/PVME blend (slow relaxation is filled triangles; fast relaxation is filled inverted triangles).

segmental times for PVME in the blend state broadens as the temperature is lowered. The breakdown of tTS is consistent for both OS and DS data for PS/PVME blends.

All DS data show the glass transition of PVME as a local maximum in tan δ_d. The dielectric loss spectrum of PVME (and the PS/PVME blend at higher temperatures) shows a sharp upturn at low frequencies (often called a "DC tail"), generally attributed to the presence of ionic impurities.[65] If this upturn is subtracted as a simple conductivity effect, the local maximum corresponding to the glass transition (the α-relaxation) is empirically described by the Havriliak−Negami (H−N) equation.[65]

$$\frac{\epsilon^*(\nu) - \epsilon_\infty + i\sigma/(\epsilon_0\nu)}{\epsilon_0 - \epsilon_\infty} = \frac{1}{[1 + (i\nu\tau_{HN})^\alpha]^\gamma} \tag{5}$$

ϵ_0 and ϵ_∞ are the limiting low- and high-frequency permittivities, σ is the DC conductivity, τ_{HN} is the H−N relaxation time, and α and γ are empirical fitting parameters ($-\alpha\gamma$ is the high-frequency slope of log ϵ'' vs log ν). For PVME, the high-temperature dielectric data are well described by eq 5 with $\alpha = 0.75$ and $\gamma = 0.55$. For the 30/70 wt % PS-130/PVME blend (Figure 3b), the dielectric data at individual temperatures are still reasonably described by eq 5, but the low-frequency side of the ϵ'' peak broadens as the temperature is lowered ($\alpha = 0.5$ at 311 K and $\alpha = 0.35$ at 261 K). The 50/50 wt % PS-50/PVME blend exhibited an even broader ϵ'' peak, which could not be fit to eq 5. This blend required assuming two H−N mode distributions to fit the dielectric response. To facilitate comparisons with literature data, we determine the relaxation time τ_{max} associated with the maximum of each mode distribution, from the H-N fitting parameters in the usual way.[66]

$$\tau_{max} = \tau_{HN}\left[\tan\left(\frac{\pi}{2(\gamma + 1)}\right)\right]^{-1/\alpha} \tag{6}$$

Figure 4 shows the temperature dependence of τ_{max} for the blends and the pure components. τ_{max} is the reciprocal of the frequency at which ϵ'' has its maximum for each H−N mode distribution. Consistent with the

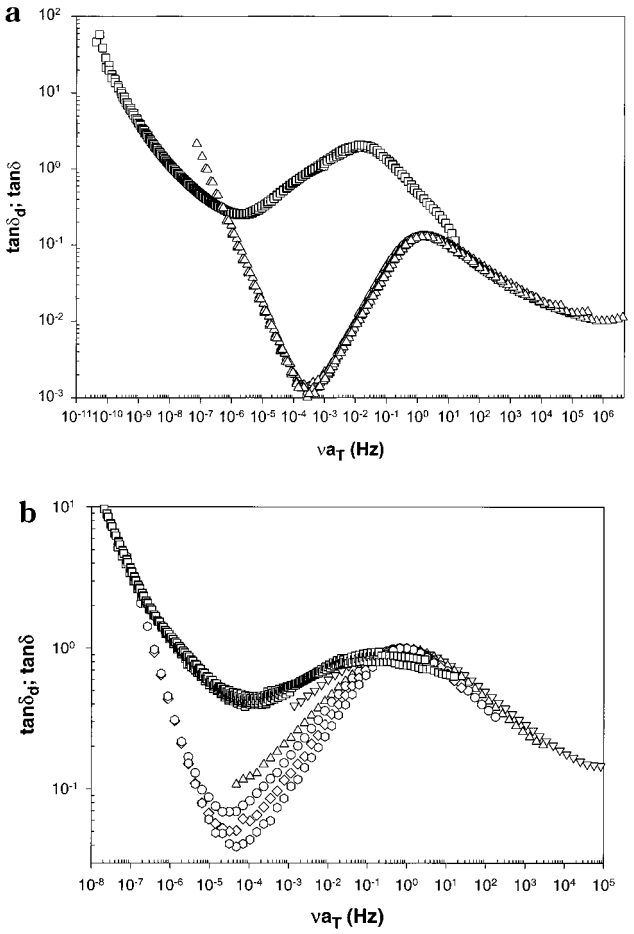

Figure 5. Comparison of dielectric and mechanical loss tangents: (a) pure PVME referenced to T_g (−24 °C) (the upper curve is OS data and lower curve is DS data) and (b) 30/70 wt % PS-130/PVME referenced to T_g (3 °C), [upper curve for OS data; the lower set of curves for DS data at −7 (inverted triangles), 3 (triangles), 13 (circles), 23 (diamonds), and 33 °C (hexagons)].

concentration fluctuation model of Kumar et al.,[13,17] the 50/50 blend exhibits a fast relaxation corresponding to nearly pure PVME and a slow relaxation that is intermediate between PS and PVME, corresponding to the average blend composition.

We contrast the DS and OS master curves of tan δ in Figure 5. Figure 5a contains the results for pure PVME, and Figure 5b presents the results for the 30/70 wt % PS-130/PVME blend. Figure 5 shows that the local maximum in tan δ, corresponding to the glass transition, occurs at a slightly higher frequency for dielectric data than for mechanical data. The failure of tTS is much more obvious in the DS data, in part because the scale is logarithmic.

6. Analysis of Shift Factors

Time−temperature superposition of tan δ data from either OS or DS is accomplished by rescaling the frequency with a shift factor a_T. For both experiments, the temperature dependence of the frequency-scale shift used to superimpose data from T to T_g is empirically described by the WLF equation.[3,67]

$$\log a_T = -C_1^g\left[\frac{T - T_g}{T - T_\infty}\right] \tag{7}$$

C_1^g is a material-specific WLF constant, referenced to the glass-transition temperature T_g, and T_∞ is the Vogel temperature (where the viscosity diverges). Williams, Landel, and Ferry used a second constant C_2^g,[3,67] with $C_2^g \equiv T_g - T_\infty$, but eq 7 is the form originally proposed by Vogel.[68] The free volume model[3] relates the frequency-scale shift factor to the fractional free volume f and its value f_g at the glass transition T_g.

$$a_T = \exp\left[B\left(\frac{1}{f} - \frac{1}{f_g}\right)\right] \tag{8}$$

B is a dimensionless parameter of order unity. This free volume model is related to the WLF equation (eq 7) by assuming that f is a linear function of temperature, and the coefficient of thermal expansion of free volume α_f is then determined by the WLF constants.[3]

$$\alpha_f = \frac{B}{C_1^g(T_g - T_\infty)\ln 10} \tag{9}$$

Figure 6a is the Vogel plot used to determine C_1^g and T_∞ from the temperature dependence of a_T used in the superposition of tan δ from OS data for pure PVME (Figure 1a). Motivated by the form of the WLF equation (eq 7), T_∞ is manually adjusted to give the best straight line in the Vogel plot.[59] This procedure for determination of WLF coefficients is the most reliable of several that have been suggested.[3] The open squares in Figure 6a are the a_T we determined from the OS data of Kannan and Lodge[69] on a highly entangled PVME ($M_w = 1.3 \times 10^6$; $M_w/M_n \cong 1.3$). Those a_T agree well with our determinations from OS for PVME (filled squares), and the linearity of both data sets gives us considerable confidence in our determinations of C_1^g and T_∞ of pure PVME from OS data. The circles in Figure 6a are the a_T from construction of the DS master curve of PVME (Figure 3a). The DS a_T do not agree with the a_T from OS. Even though tTS works reasonably for PVME in both types of data, the temperature dependence of relaxation depends on whether the relaxation is probed dielectrically or mechanically, as has been reported for many homopolymers.[70−77]

Figure 6b is the corresponding Vogel plot used to determine C_1^g and T_∞ from the a_T used to construct the master curve for tan δ_d from the DS data for pure PVME (Figure 2a). The linearity of these data (circles) shows that the dielectric frequency-scale shift factors are also described well by the WLF equation (eq 7), but the mechanical data (open and filled squares) are clearly not described by the same WLF coefficients that work for the DS data.

In Figure 6c, we compare the frequency-scale shift factors (a_T) for our polystyrenes with those of Plazek[61] in a Vogel plot. This plot uses Plazek's values of T_g and T_∞ (see Table 2). Since Plazek studied temperatures much closer to T_g, his determination of T_∞ is considerably more reliable. The discrepancy between our a_T and those of Plazek is beyond experimental error and the reason for this discrepancy is not clear.

The WLF coefficients, Vogel temperatures, and the coefficients of thermal expansion of free volume for the PS and PVME pure components are shown in Table 2. In the calculation of α_f, we set $B = 1$ as suggested by Ferry,[3] because B is known to be of order unity and cannot be separated from α_f without an independent measure of free volume. The larger Vogel temperature

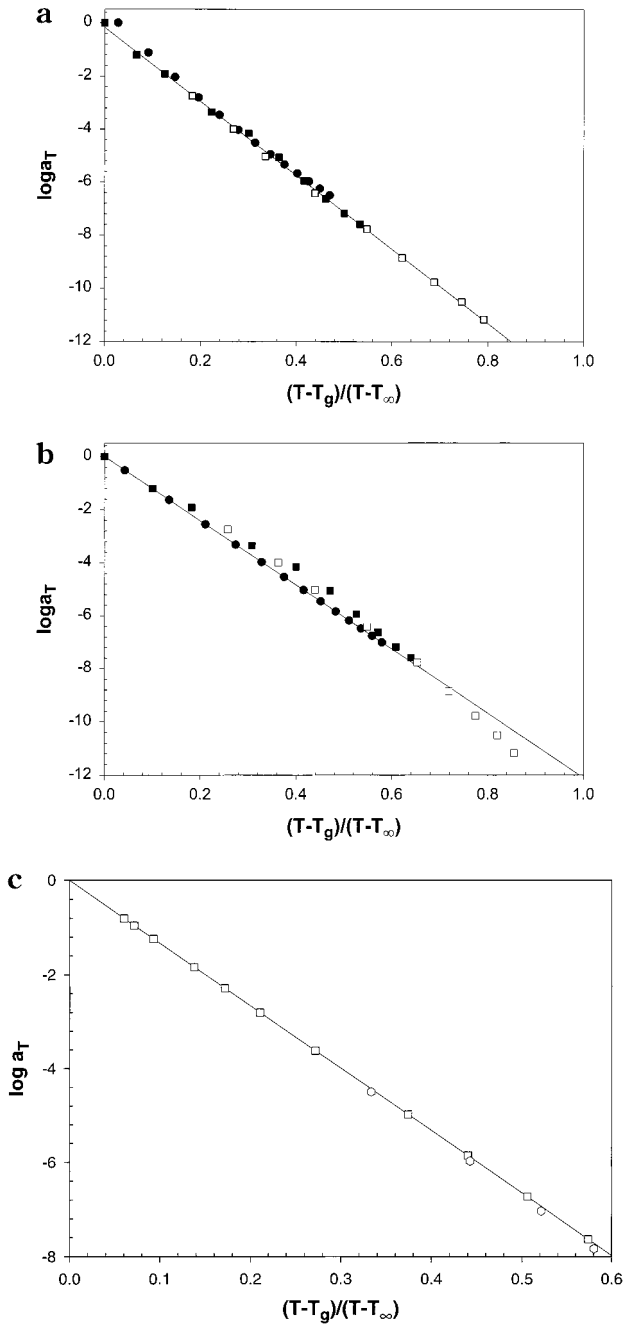

Figure 6. Vogel plots for pure components: (a) best fit to PVME OS data *only* ($T_g = -24$ °C and $T_\infty = -94$ °C), (b) best fit to PVME DS data *only* ($T_g = -24$ °C and $T_\infty = -69$ °C) using our OS data (filled squares), the OS data of Kannan and Lodge[69] (open squares), and the DS data (filled circles), and (c) comparison of shift factors for our OS data on PS-50 ($M_w =$ 56 000, hexagons) with Plazek's creep data[61] on pure PS (M_w = 46 900, squares). All lines are regression fits to eq 7.

Table 2. Thermal Properties of Pure Polymers

polymer	method	T_g (°C)	C_1^g	T_∞ (°C)	$10^4\alpha_f$ (K^{-1})
PVME	OS	−24	13.9	−94	4.5
PVME	DS	−24	12.1	−69	8.0
PS-50	OS	104	11.5	58	8.2
PS-130	OS	106	11.6	58	6.7
PS-260	OS	106	11.7	58	7.7
PS [61]	creep	97	12.7	50	7.3

T_∞ and the larger coefficient of thermal expansion of the free volume α_f, observed dielectrically for PVME, indicate that the dielectric relaxation processes have a stronger temperature dependence than the mechanical

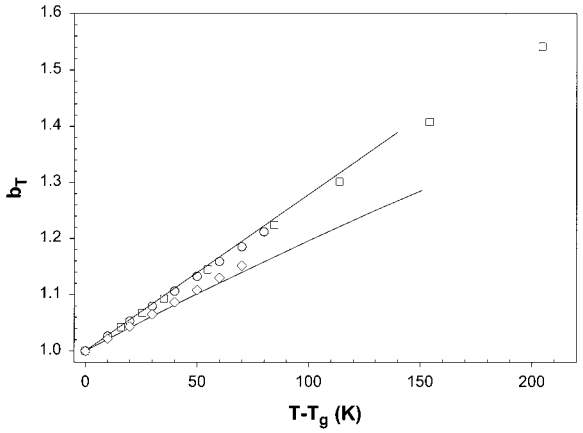

Figure 7. Temperature dependence of modulus-scale shift factors (b_T): PVME using our data (circles), the data of Lodge and Kannan[69] (squares), and polystyrenes (diamonds; PS-50, PS-130, and PS-260 data all agree). Solid curves are the Rouse model predictions (lower curve for PS; upper curve for PVME).

relaxation processes. This statement is consistent with the trends seen in Figure 6 and is observed for many other homopolymers in the literature.[70−77] The segmental and terminal relaxations of polymers have different temperature dependences.[78] DS only probes PVME's segmental modes, whereas OS is influenced by both segmental and terminal relaxation processes. Identical WLF parameters for dielectric, mechanical, and incoherent quasielastic neutron scattering data of pure PVME were reported in previous work by Colmenero et al.,[79] but that work only covered a very limited range of temperatures for mechanical data (between −30 and 0 °C).

Although the discrepancies between the a_T's used in DS and OS are beyond experimental error, they are small, as judged in Figure 6a. However, these small differences lead to a *25 K difference in Vogel temperatures* from DS and OS of pure PVME. This 25 K difference is far beyond the experimental uncertainty in T_∞ of ±3 K. The T_∞ obtained for PVME from DS is consistent with the $T_\infty = -67$ °C reported by Colmenero et al. (based on their DS experiments).[80]

The temperature dependence of the modulus-scale shift factor b_T for pure PVME and pure PS is plotted in Figure 7. The b_T's for both PVME and PS appear to obey the Rouse prediction ($b_T \sim \rho T$, with ρ the temperature-dependent density and T the absolute temperature), using literature PVT data for PVME[40] and for PS.[81]

7. Discussion

Kannan and Lodge[69] used OS to study a high molecular weight PVME ($M_w = 1.3 \times 10^6$) and found that the plateau modulus of PVME is $G_N^0 = 4.07 \times 10^6$ dynes/cm^2 at 30 °C. Using $\rho = 1.01$ g/cm^3, we calculate the molecular weight of an entanglement strand $M_e = \rho RT/G_N^0 = 6250$ in a PVME melt. Using the Kuhn segment length for PVME[34] ($b = 6.9$ Å), we calculate the tube diameter $a = b[\rho RT/(M_K G_N^0)]^{1/2}$ of the reptation model[82] to be $a_{PVME} = 47$ Å for PVME, where $M_K = 130$ is the molecular weight of a Kuhn segment. Since PS has a larger tube diameter[82] ($a_{PS} = 82$ Å), we expect the PVME will become progressively less entangled as PS is added. Assuming a single tube in the blend[11] leads to a simple blending law for the effective tube diameter as a function of the volume fraction of PVME, ϕ.

$$\frac{1}{a} = \frac{\phi}{a_{\mathrm{PVME}}} + \frac{(1-\phi)}{a_{\mathrm{PS}}} \tag{10}$$

The tube model relates a chain's terminal relaxation time τ to the time scale of motion of a Kuhn segment τ_0. The Doi fluctuation model[83] gives the following expression for the ratio of relaxation times.

$$\frac{\tau}{\tau_0} \cong \frac{N^3}{N_e}\left[1 - \left(\frac{N_e}{N}\right)^{1/2}\right]^2 \tag{11}$$

N is the number of Kuhn segments per chain, and N_e is the number of Kuhn segments per entanglement strand. Terminal relaxation of the chain is faster than the standard reptation result (N^3/N_e) by a simple fluctuational correction. Equation 11 should apply for the ratio of relaxation times in a blend, as well as in a pure component melt, provided that the entanglement strand length is adjusted accordingly. At any constant composition ϕ, the entanglement strand length is constant, and the ratio of relaxation times has a slightly stronger than cubic dependence on chain length (roughly $\tau/\tau_0 \sim N^{3.4}$). An example of the use of eq 11 to determine τ_0 from τ is shown in Figure 1a for PVME. Also shown is the Rouse time of an entanglement strand $\tau_e = \tau_0 N_e^2$. Notice that τ and τ_e correspond to crossing points of G' and G''. The relaxation time of the Kuhn segment τ_0 does not generally correspond to the high-frequency crossing point of G' and G'', because the high-frequency relaxations associated with the glass transition depend on the chemical details of the polymer chain. We shall see below that τ_0 corresponds to the long-time end of the segmental relaxation time distribution.

The terminal relaxation times τ, estimated from the terminal (low-frequency) crossing point of G' and G'', are plotted in Figure 8 as a function of temperature. We need to particularly focus our attention on the three 30/70 wt % PS/PVME blends (filled symbols). If the terminal relaxation were solely due to the PVME chains, we would expect the terminal relaxation time to be insensitive to PS chain length.[84] On the other hand, if the terminal relaxation in the blends were due to PS alone, eq 11 predicts the terminal time to scale as the 3.4 power of PS chain length, which thus should have a chain length dependence similar to the three pure PS samples shown in Figure 8. The observed PS chain length dependence of the terminal relaxation time in the blend lies between these results, indicating that both PVME and PS chains are relaxing in the vicinity of the terminal peak in the loss modulus.

Since the terminal relaxation of the three 30/70 wt % PS/PVME blends has a weak dependence on PS chain length ($\tau \sim M_{\mathrm{PS}}^{1.6}$), we suspect that the blended PVME chains relax more slowly than the PS-50 chains and more rapidly than the PS-260 chains and at about the same rate as the PS-130 chains. This crossover explains the weak dependence of the terminal relaxation time on PS chain length seen in Figure 8, as well as the fact that there is no obvious second terminal relaxation. There is a hint of a second terminal relaxation in tan δ near 10^{-6} rad/s in Figure 2b that likely corresponds to the relaxation of PVME in the blend with PS-260. There is no trace of any second relaxation in either the 30/70 wt % PS-130/PVME blend (Figure 2a) or the 30/70 wt % PS-50/PVME blend.[85] Miscible blends of narrow molecular weight distribution polymers typically have two local maxima in their terminal loss modulus.[4,6,7,11,13]

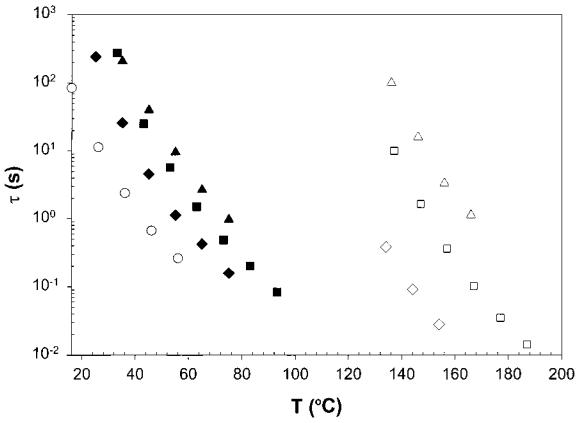

Figure 8. Temperature dependence of terminal relaxation times: PVME (open circles), PS-50 (open diamonds), PS-130 (open squares), PS-260 (open triangles), 30/70 wt % PS-50/PVME (filled diamonds), 30/70 wt % PS-130/PVME (filled squares), and 30/70 wt % PS-260/PVME (filled triangles).

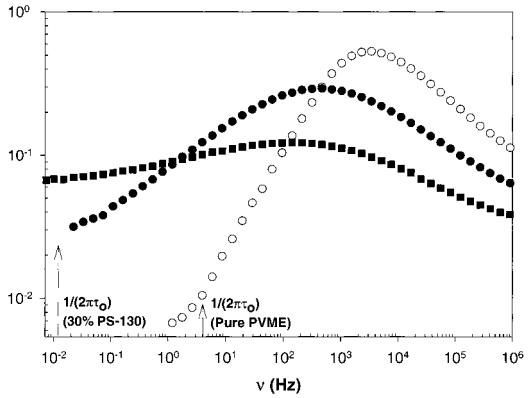

Figure 9. Comparison of the dielectric loss spectra: pure PVME at 3 °C (open circles), 30/70 wt % PS-130/PVME blend at 3 °C (filled circles), and 50/50 wt % PS-50/PVME blend at 5 °C (squares). The left and right arrows denote the Kuhn segment relaxation frequency in the 30/70 wt % PS-130/PVME blend and pure PVME, respectively.

The exception to this rule, of course, comes when the two components happen to have similar terminal relaxation times in the blend.[10] In practice, the times must be separated by more than an order of magnitude to resolve to two peaks in the OS experiment.

Figure 9 compares the dielectric response of the pure PVME at 3 °C, the 30/70 wt % PS/PVME blend at 3 °C (the blend T_g), and the 50/50 wt % PS/PVME blend at 5 °C. The broadening of the dielectric loss in the blend state is evident. This broadening has been observed for many miscible blends and is ascribed to the presence of concentration fluctuations.[14,15,23,55] The PVME segments find themselves in a wide variety of environments when blended with PS, spanning a range from the pure PVME to regions with longer relaxations that are slowed by surrounding PS chains.

Using eq 11, we estimate the effective time scale of motion of a Kuhn segment τ_0 from the terminal relaxation time τ for PVME in both the PVME melt state and the 30/70 wt % PS/PVME blend state at 3 °C. In the case of the blend, the terminal time was estimated by extrapolation of the frequency at which $G' = G''$ from higher temperature data using the WLF equation. The Kuhn segment relaxation times are shown as the arrows in Figure 9. Clearly, at low temperatures, the effective time scale for free motion of Kuhn segments τ_0 *is near the long-time end of the distribution of segmental times.*

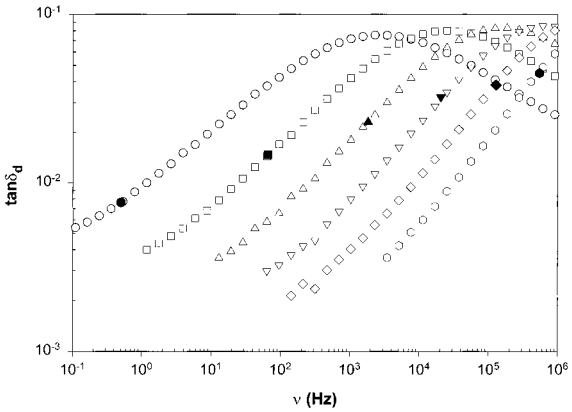

Figure 10. Dielectric loss tangent of 30/70 wt % PS-130/PVME at different temperatures: 8 (circles), 18 (squares), 28 (triangles), 38 (inverted triangles), 48 (diamonds), and 58 °C (hexagons). The filled symbol at each temperature is the frequency $[1/(2\pi\tau_0)]$ corresponding to the effective time scale of motion of a Kuhn segment τ_0, calculated from the terminal relaxation time τ, using eq 11.

The temperature dependence of the dielectric loss tangent for the 30/70 wt % PS/PVME blend is shown in Figure 10. The filled symbols in Figure 10 represent the frequency $[1/(2\pi\tau_0)]$ associated with the effective time scale of motion of a Kuhn segment τ_0, calculated from the terminal relaxation time τ, using eq 11. As the temperature is lowered, the spectrum of segmental relaxation times broadens and shifts to lower frequency. The effective Kuhn segment motion time corresponds to a progressively longer time in that distribution as it broadens. This observation is quite consistent with the "cooperative volume" theory of the glass transition.[86−89] The premise of this theory is that motion is restricted within the cooperative volume until the entire volume can move in some cooperative manner. The size of the cooperative volume grows as the temperature is lowered, which acts to retard relaxation. In weakly interacting blends with large ΔT_g (such as PS/PVME), concentration fluctuations create a variety of local compositions, each with its own cooperative volume.[17] The distribution of segmental times broadens as the temperature is lowered because fluctuations rich in the high T_g polymer get larger (and slower) cooperative volumes.

For terminal relaxation, the chain must reptate out of its confining tube. The fluctuations rich in the high T_g polymer act as pinning points along the tube, controlling the effective friction coefficient for terminal relaxation or the effective time scale of motion of a Kuhn segment τ_0. Thus, τ_0 moves further toward the long-time end of the distribution of segmental relaxation times when the largest cooperative volumes get larger (as the temperature is lowered).

8. Conclusions

We have used dielectric spectroscopy and oscillatory shear to study the temperature dependence of relaxations in PVME, PS, and their blends. We find that the empirical time−temperature superposition principle works reasonably for PVME, approximately for PS with $T > T_g + 10$ K, and fails for PS/PVME blends at all temperatures studied ($T_g \leq T \leq T_g + 90$ K). Superposition of tan δ is necessary for deciding whether tTS works, as done by Cavaille et al.[43] and Stadler et al.,[45] for PS/PVME blends. Superposition of G' and G'' can lead to an erroneous conclusion of thermorheological simplicity. Use of the loss tangent $\tan\delta \equiv G''/G'$ obviates the modulus-scale shift, which imparts an additional degree of freedom that can allow tTS to appear valid when shifting G' and G''.

We used a simple tube model to make quantitative comparisons between the distribution of segmental relaxation times (probed by DS) and the apparent time scale for free motion of a Kuhn segment (calculated from eq 11, using the terminal time from OS). At low temperatures, free motion of a Kuhn segment (the shortest Rouse mode of the chain) occurs at the long-time end of the spectrum of segmental relaxation times. This finding is particularly important for miscible blends with weak interactions between components, where the distribution of segmental relaxation times is anomalously broadened by concentration fluctuations[15,17] in a temperature-dependent manner.

Acknowledgment. Financial support of this research from the National Science Foundation through Grant DMR-9629901 is acknowledged with gratitude. R.J. is indebted to the Services Fédéraux des Affaires Scientifiques, Techniques et Culturelles (PAI 4/11) for general support to CERM. We thank Reimund Stadler and Timothy E. Long for having synthesized two of the polystyrene samples used in this work. We thank Michael R. Landry for DSC results. We also thank Timothy P. Lodge for sending his OS data on PVME and Sanat K. Kumar for discussions.

References and Notes

(1) Paul, D. R.; Newman, S. *Polymer Blends*, volume 1. Academic Press: New York, 1978.
(2) Utracki, L. A. *Polymer Alloys and Blends: Thermodynamics and Rheology*; Carl Hanser Verlag: Munich, 1990.
(3) Ferry, J. D. *Viscoelastic Properties of Polymers*, 3rd ed.; Wiley: New York, 1980.
(4) Colby, R. H. *Polymer* **1989**, *30*, 1275−1278.
(5) Roland, C. M.; Ngai, K. L. *Macromolecules* **1991**, *24*, 2261−2265.
(6) Roovers, J.; Toporowski, P. M. *Macromolecules* **1992**, *25*, 1096−1102.
(7) Roovers, J.; Toporowski, P. M. *Macromolecules* **1992**, *25*, 3454−3461.
(8) Chung, G. C.; Kornfield, J. A.; Smith, S. D. *Macromolecules* **1994**, *27*, 964−973.
(9) Chung, G. C.; Kornfield, J. A.; Smith, S. D. *Macromolecules* **1994**, *27*, 5729−5741.
(10) Arendt, B. H.; Kannan, R. M.; Zewail, M.; Kornfield, J. A.; Smith, S. D. *Rheol. Acta* **1994**, *33*, 322−336.
(11) Zawada, J. A.; Fuller, G. G.; Colby, R. H.; Fetters, L. J.; Roovers, J. *Macromolecules* **1994**, *27*, 6861−6870.
(12) Arendt, B. H.; Krishnamoorti, R.; Kornfield, J. A.; Smith, S. D. *Macromolecules* **1997**, *30*, 1127−1137.
(13) Pathak, J. A.; Colby, R. H.; Kamath, S. Y.; Kumar, S. K.; Stadler, R. *Macromolecules* **1998**, *31*, 8988−97.
(14) Roland, C. M.; Ngai, K. L. *Macromolecules* **1992**, *25*, 363−367.
(15) Zetsche, A.; Fischer, E. W. *Acta Polymer* **1994**, *45*, 168−175.
(16) Ngai, K. L.; Roland, C. M. *Macromolecules* **1995**, *28*, 4033−35.
(17) Kumar, S. K.; Colby, R. H.; Anastasiadis, S. H.; Fytas, G. *J. Chem. Phys.* **1996**, *105*, 3777−3788.
(18) Alvarez, F.; Alegria, A.; Colmenero, J. *Macromolecules* **1997**, *30*, 597−604.
(19) Alegria, A.; Colmenero, J.; Ngai, K. L.; Roland, C. M. *Macromolecules* **1994**, *27*, 4486−92.
(20) Hadziioannou, G.; Stein, R. S. *Macromolecules* **1984**, *17*, 567−573.
(21) Han, C. C.; Bauer, B. J.; Clark, J. C.; Muroga, Y.; Matsushita, Y.; Okada, M.; Tran-Cong, Q.; Chang, T.; Sanchez, I. C. *Polymer* **1988**, *29*, 2002−2014.
(22) Han, C. C. *Rubber Chem. Tech.* **1990**, *63*, 98−109.

(23) Zetsche, A.; Kremer, F.; Jung, W.; Schulze, H. *Polymer* **1990**, *31*, 1883−1887.
(24) Bank, M.; Leffingwell, J.; Thies, C. *Macromolecules* **1971**, *4*, 43−46.
(25) Bank, M.; Leffingwell, J.; Thies, C. *J. Polym. Sci., Part A-2* **1972**, *10*, 1097−1109.
(26) Nishi, T.; Kwei, T. *Polymer* **1975**, *16*, 285−290.
(27) Davis, D. D.; Kwei, T. K. *J. Polym. Sci.: Polym. Phys. Ed.* **1980**, *18*, 2337−2345.
(28) Cimmino, S.; Pace, E. D.; Martuscelli, E.; Silvestre, C.; Rice, D. M.; Karasz, F. E. *Polymer* **1993**, *34*, 214−217.
(29) Amelino, L.; Martuscelli, E.; Sellitti, C.; Silvestre, C. *Polymer* **1990**, *31*, 1051−1057.
(30) Mirau, P. A.; Tanaka, H.; Bovey, F. A. *Macromolecules* **1988**, *21*, 2929−2933.
(31) Mirau, P. A.; Bovey, F. A. *Macromolecules* **1990**, *23*, 4548−4552.
(32) Mirau, P. A.; White, J. L. *Magn. Resn. Chem.* **1994**, *32*, S23−S29.
(33) Herkt-Maetzky, C.; Schelten, J. *Phys. Rev. Lett.* **1983**, *51*, 896−899.
(34) Shibayama, M.; Yang, H.; Stein, R. S.; Han, C. C. *Macromolecules* **1985**, *18*, 2179−2187.
(35) Yang, H.; Shibayama, M.; Stein, R. S.; Shimizu, N.; Hashimoto, T. *Macromolecules* **1986**, *19*, 1667−1674.
(36) Schwahn, D.; Mortensen, K.; Yee-Madeira, H. *Phys. Rev. Lett.* **1987**, *58*, 1544−1546.
(37) Schwahn, D.; Mortensen, K.; Springer, T.; Yee-Madeira, H.; Thomas, R. *J. Chem. Phys.* **1987**, *87*, 6078−6087.
(38) Brereton, M. G.; Fischer, E. W.; Herkt-Maetzky, C.; Mortensen, K. *J. Chem. Phys.* **1987**, *87*, 6144−6149.
(39) Takeno, H.; Koizumi, S.; Hasegawa, H.; Hashimoto, T. *Macromolecules* **1996**, *29*, 2440−2448.
(40) Shiomi, T.; Hamada, F.; Nasako, T.; Yoneda, K.; Imai, K.; Nakajima, A. *Macromolecules* **1990**, *23*, 229−233.
(41) Tsujita, Y.; Kato, M.; Kinoshita, T.; Takizawa, A. *Polymer* **1992**, *33*, 773−777.
(42) Brekner, M. J.; Cantow, H. J.; Schneider, H. A. *Polymer. Bull.* **1985**, *14*, 17−24.
(43) Cavaille, J. Y.; Corrinne, J.; Perez, J.; Monnerie, L.; Johari, G. P. *J. Polym. Sci., Part B: Polym. Phys.* **1987**, *25*, 1235−1251.
(44) Ajji, A.; Choplin, L.; Prud'Homme, R. E. *J. Polym. Sci., Part B: Polym. Phys.* **1988**, *26*, 2279−2289.
(45) Stadler, R.; Freitas, L. D. L.; Krieger, V.; Klotz, S. *Polymer* **1988**, *29*, 1643−1647.
(46) Schneider, H. A.; Wirbser, J. *New Polym. Mater.* **1990**, *2*, 149−166.
(47) Ajji, A.; Choplin, L.; Prud'Homme, R. E. *J. Polym. Sci., Part B: Polym. Phys.* **1991**, *29*, 1573−1578.
(48) Ajji, A.; Choplin, L. *Macromolecules* **1991**, *24*, 5221−5223.
(49) Kitade, S.; Takahashi, Y.; Noda, I. *Macromolecules* **1994**, *27*, 7397−7401.
(50) Takahashi, Y.; Suzuki, H.; Nakagawa, Y.; Noda, I. *Macromolecules* **1994**, *27*, 6476−6481.
(51) Kapnistos, M.; Hinrichs, A.; Vlassopoulos, D.; Anastassiadis, S.; Stammer, A.; Wolf, B. A. *Macromolecules* **1996**, *29*, 7155−7163.
(52) Kapnistos, M.; Vlassopoulos, D.; Anastasiadis, S. H. *Europhys. Let.* **1996**, *34*, 513−518.
(53) Green, P. F.; Adolf, D. B.; Gilliom, L. R. *Macromolecules* **1991**, *24*, 3377−3382.
(54) Green, P. F. *Macromolecules* **1991**, *24*, 3373−3376.
(55) Roland, C. M.; Ngai, K. L. *Prog. Colloid Polym. Sci.* **1993**, *91*, 75−79.
(56) Schmidt-Rohr, K.; Clauss, J.; Spiess, H. W. *Macromolecules* **1992**, *25*, 3273−77.
(57) Tezuka, A.; Takegoshi, K.; Hikichi, K. *J. Molec. Struct.* **1995**, *355*, 1−7.
(58) Miyamoto, M.; Sawamoto, M.; Higashimura, T. *Macromolecules* **1984**, *17*, 265; 2228.
(59) Plazek, D. J. *J. Polym. Sci., Part B: Polym. Phys. Ed.* **1982**, *20*, 729−742.
(60) Plazek, D. J.; Rosner, M. J.; Plazek, D. L. *J. Polym. Sci., Part B: Polym. Phys.* **1988**, *26*, 473−489.
(61) Plazek, D. J. *J. Phys. Chem.* **1965**, *69*, 3480−3487.
(62) Plazek, D. J. *J. Rheol.* **1996**, *40*, 987−1014.
(63) McCrum, N. G.; Read, B. E.; Williams, G. *Anelastic and Dielectric Effects in Polymeric Solids*; Dover Publications, Inc.: New York, 1967.
(64) Debye, P. *Polar Molecules*. Chemical Catalog Company, Inc.: New York, 1929.
(65) Havriliak, S.; Havriliak, S. J. *Dielectric and Mechanical Relaxations in Materials*: Carl Hanser Verlag: Munich, 1997.
(66) Alvarez, F.; Alegria, A.; Colmenero, J. *Phys. Rev. B* **1991**, *44*, 7306−12.
(67) Williams, M. L.; Landel, R. F.; Ferry, J. D. *J. Am. Chem. Soc.* **1955**, *77*, 3701−3707.
(68) Vogel, H. *Physik. Z.* **1921**, *22*, 645−6.
(69) Kannan, R. M.; Lodge, T. P. *Macromolecules* **1997**, *30*, 3694−3695.
(70) Floudas, G.; Fytas, G.; Fischer, E. W. *Macromolecules* **1991**, *24*, 1955−61.
(71) Plazek, D. J.; Zheng, X. D.; Ngai, K. L. *Macromolecules* **1992**, *25*, 4920−24.
(72) Plazek, D. J.; Schlosser, E.; Schonhals, A.; Ngai, K. L. *J. Chem. Phys.* **1993**, *98*, 6488−6491.
(73) Schonhals, A. *Macromolecules* **1993**, *26*, 1309−12.
(74) Plazek, D. J.; Bero, C. A.; Neumeister, S.; Floudas, G.; Fytas, G.; Ngai, K. L. *Colloid Polym. Sci.* **1994**, *272*, 1430−38.
(75) Santangelo, P. G.; Ngai, K. L.; Roland, C. M. *Macromolecules* **1996**, *29*, 3651−53.
(76) Santangelo, P. G.; Roland, C. M. *Macromolecules* **1998**, *31*, 3715−19.
(77) Nicolai, T.; Floudas, G. *Macromolecules* **1998**, *31*, 2578−85.
(78) Plazek, D. J.; O'Rourke, V. M. *J. Polym. Sci., Part A-2* **1971**, *9*, 209−243.
(79) Colmenero, J.; Alegria, A.; Alberdi, J. M.; Alvarez, F.; Frick, B. *Phys. Rev. B* **1991**, *44*, 7321−29.
(80) Alegria, A.; Elizetxea, C.; Cendoya, I.; Colmenero, J. *Macromolecules* **1995**, *28*, 8819−8823.
(81) Zoller, P.; Walsh, D. J. *Standard Pressure−Volume−Temperature Data for Polymers*; Technomic: Lancaster, PA, 1995.
(82) Doi, M.; Edwards, S. F. *The Theory of Polymer Dynamics*; Clarendon Press: Oxford, 1986.
(83) Doi, M. *J. Polym. Sci., Polym. Lett. Ed.* **1981**, *19*, 265−273.
(84) Rubinstein, M.; Colby, R. H. *J. Chem. Phys.* **1988**, *89*, 5291−5306.
(85) Pathak, J. A. Master's Thesis, Pennsylvania State University, University Park, PA.
(86) Adam, G.; Gibbs, J. H. *J. Chem. Phys.* **1965**, *43*, 139−146.
(87) Donth, E. J. *J. Non-Cryst. Solids* **1991**, *131−133*, 204−206.
(88) Donth, E. J. *Relaxation and Thermodynamics in Polymers*; Akademie Verlag: Berlin, 1992.
(89) Matsuoka, S. *Relaxation Phenomena in Polymers*; Hanser: New York, 1992.

MA9817121